

Modeling of High Temperature Thermosyphons

André Felipe Vieira da Cunha^{*} and Márcia B. H. Mantelli[†]

Heat Pipe Laboratory (LABTUCAL/LEPTEN) Florianópolis, Santa Catarina, 88036-900, Brazil

Nomenclature

A_p, A_s, A_n and B	=	coefficient of approach equation
A	=	area
c_p	=	specific heat at constant pressure
h	=	heat transfer coefficient
h_v	=	latent heat of vaporization
g	=	gravity
k	=	thermal conductivity
L	=	length
\dot{m}	=	mass flow rate
P	=	pressure
Pr	=	Prandtl number, $Pr = C_p \mu / k$
q	=	heat flux
Q	=	heat flux rate
r	=	radius
Re	=	Reynolds number
T	=	temperature
x	=	the axial distance between the top of film liquid and the condenser bottom

Greek symbols

ρ	=	density
δ	=	thickness of film liquid
μ	=	viscosity
σ	=	surface tension
Δx	=	length of control volume

Subscripts

atm	=	atmosphere
c	=	condenser
e	=	evaporator
e'	=	east
ext	=	external
f	=	film
p	=	pool
i	=	inside
l	=	liquid
v	=	vapor
sat	=	saturated
t	=	total and transversal
w	=	wall
w'	=	west

^{*} Mechanical Engineering Department, Federal University of Santa Catarina, andre@labsolar.ufsc.br.

[†] Associate Fellow AIAA, Mechanical Engineering Department, Federal University of Santa Catarina, marcia@emc.ufsc.br.

1. Introduction

Thermosyphons are devices with high thermal conductivity that can transfer high quantities of heat. In its most simple form, a thermosyphon is a hollow evacuated metal pipe, charged with a pre-determined amount of an appropriate working fluid. It can be divided into three main sections: evaporator, where the heat is delivered to the device, an adiabatic section (which can or can not exist) and a condenser, where the heat is released. The heat causes the evaporation of the working fluid and the vapor, by means of pressure gradients, go toward the condenser region, where it condenses, returning to the evaporator by gravity.

High-temperature thermosyphons can be applied in regenerative heat exchangers in petroleum plants, where high temperature streams (above 400° C) are released to atmosphere from furnaces. The use of this energy, to preheat air in industrial furnaces, represents a good example of recoverable thermal energy. The development of new heat pipe technology will enable the increase of the energetic efficiency of industrial processes.

A description of high temperature heat pipes can be found in several books, including Faghri [1] and Dunn and Reay [2]. Storey [3] and Reed [4] present numerical and analytical models, respectively, for thermosyphons. In the present work, a different model is introduced, which is solved by means of a numerical iterative methods and it is based in the Nusselt's film condensation hypothesis for condensation in the condenser region and boiling in the evaporator.

2. High temperature thermosyphon

High temperature thermosyphons work at temperatures above 400°C. The working fluid consists of a liquid metal such as mercury, sodium, lithium or potassium. The tube material (metal) must be chemically compatible with the working fluid, to avoid chemical reactions, which could produce undesirable non condensable gases. The material of the tubes must also resist to corrosion, while it keeps its mechanical properties at the high working temperatures. The manufacture of this device is also challenging and demands careful, well determined procedures.

2.1. Material mechanical limits

Thermosyphons for operation at temperatures above about 830°C are typically constructed with refractory metals such as tungsten, molybdenum and some special steel. The use of these materials is not a restriction for applications in space where the environment is at high vacuum and where material and fabrication costs do not constitute a severe constraint. However, for high temperature industrial applications, the operation environment is usually highly oxidizing or otherwise corrosive and costs are the dominant consideration.

One of the main concerns about the technology of high temperature heat recovery equipments is related to the temperature working limits of the materials used in heat exchangers. Heat exchangers made of stainless steel, for example, can not exceed 700 °C. When subjected to high temperatures, all metallic alloys get weaker and decrease their stiffness. Consequently, the tubes made of this material are limited to applications where they are subjected to small pressure differences. Figure 1 shows the operation limits of materials that are in current use in heat exchangers. An alternative approach is to construct thermosyphons made of ceramic tubing which, in this case, full advantage can be taken of the high temperature strength and of the excellent corrosion and erosion resistances of selected ceramic materials, including silicon carbide and alumina.

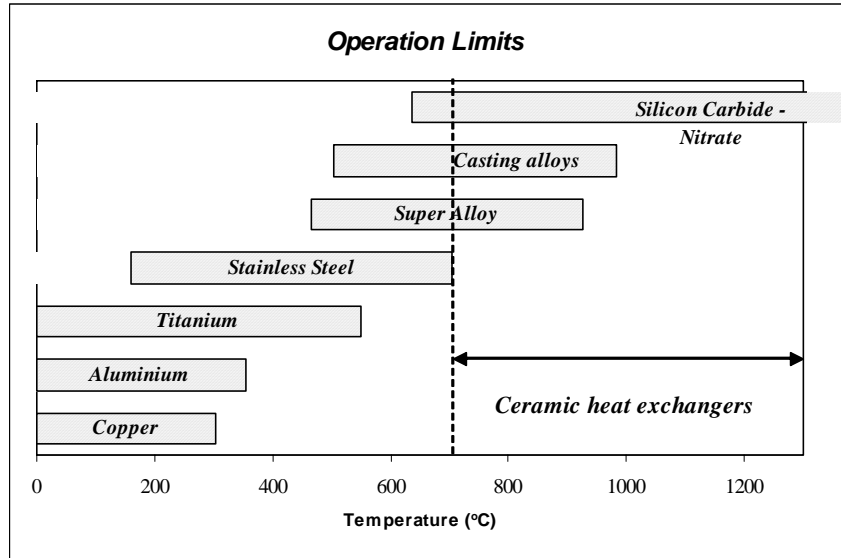


Figure 1 Operation limit of materials in heat exchangers

2.2. Working fluids

The working fluid used in thermosyphons must be selected to match the operation temperature range of interest. For high temperature thermosyphons, the usual working fluids are liquid metal including potassium, sodium or lithium. Table 1 shows the melting and boiling points, and the usual range of operation of some liquid metals.

These liquid metals are excellent for heat transfer, having a high conductivity, high heats of vaporization, and a good surface tension coefficient. However, in general, some of them, as lithium, are not compatible with ceramic materials (Ranken [11]). A ceramic pipe is therefore provided with a protective inner liner which matches the ceramic expansion characteristics. Stainless steel and Inconel are materials appropriate to be used with these working fluids.

Table 1. Melting and boiling points of liquid metals at atmosphere pressure (1 atm).

Working Fluids	Melting Point	Boiling Point	Usual Range
Sodium	98 °C	892 °C	600 up to 1200 °C
Lithium	179 °C	1340 °C	1000 up to 1800 °C
Potassium	62 °C	774 °C	500 up to 1000 °C
Mercury	-39 °C	357 °C	300 up to 600 °C

Sodium, potassium and lithium are elements that require careful handling because they are highly reactive with water and humidity, liberating flammable gases. Potassium reacts with water and humidity to form explosive mixtures with air at normal temperature, for example.

Yamamoto et al. [5] analyzed experimentally heat pipes with mercury as a working fluid. Despite presenting good thermal performance, mercury is a highly toxic substance and has been avoided in thermosyphons for industrial applications. They are, however, considered a reasonable option for academic study purposes.

3. Proposed model

A preliminary steady state model for the temperature distribution of high temperature thermosyphons is proposed with the objective of giving insight in the performance of this device. Figure 2 shows a schematic of the physical

model adopted, where the thermosyphon is divided into seven regions. Region 1 encompasses the condensed liquid film in the inner face of the condenser wall. Region 3 includes the liquid film that is in contact with the evaporator internal wall. Region 2, located within the adiabatic region, is considered thermally isolated from the environment and includes the condensed liquid which leaves the condenser. Region 4 encompasses the liquid pool under the effect of the incoming heat. The vapor inside the thermosyphon is considered to be within Region 5. All the non condensable gases eventually present in the system are considered to be within the Region 6. Finally the Region 7 includes the metallic pipe wall.

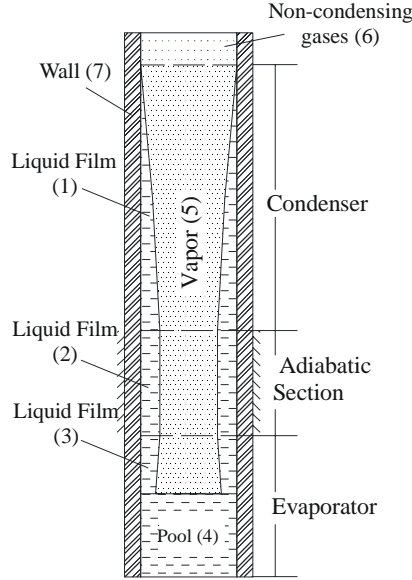


Figure 2. Schematic of the physical model for the high temperature thermosyphon.

3.1. Condenser

Models or correlations which consider the flow of condensed metal inside vertical tube walls are hard to find in the literature. In the present paper, the classical Nusselt model is considered. It is assumed that the ratio between the film thickness and tube diameter is very small ($\delta/D \ll 1$). Therefore, the inside vertical tube wall is considered a plain vertical surface and the condensed film is pushed to the condenser direction by means of the gravity. The vapor is assumed to be at the saturated temperature and no shear forces are considered. The temperatures of the saturated vapor (T_{sat}) and of the wall (T_w) are considered steady.

According to the Nusselt model (Nusselt apud Incropera [6]) that assumes: laminar flow and constant properties in the film liquid, pure vapor with uniform temperature (T_{sat}) and no shear stresses in the interface liquid-vapor, the film thickness $\delta(x)$ is given by the expression:

$$\delta(x) = \left[\frac{4k_l \mu_l (T_{sat} - T_w) x}{g \rho_l (\rho_l - \rho_v) h_{lv}} \right]^{1/4}, \quad (1)$$

where k_l is the thermal conductivity, μ_l is the viscosity, ρ_l is the density of the liquid respectively, ρ_v is the density of the vapor, h_{lv} is the liquid-vapor latent heat of evaporation and g is the gravity constant.

The film mean heat transfer coefficient \bar{h}_l is determined by the integration of local heat transfer coefficient, $h_x = k/\delta$, over the condenser length L_c , resulting in:

$$\bar{h}_L = \frac{1}{L_c} \int_0^{L_c} h dx \longrightarrow \bar{h}_L = 0,943 \left[\frac{\rho_l g (\rho_l - \rho_v) h_{lv}' k_l^3}{\mu_l (T_{sat} - T_w) L_c} \right]^{1/4}, \quad (2)$$

where $h_{lv}' = h_{lv} + 0,68 C_{p_l} (T_{sat} - T_w)$ and C_{p_l} is the liquid heat capacity.

Finally, the mass flow rate of liquid leaving the condenser (\dot{m}_{lc}), determined using the velocity profile of the falling liquid, is given by:

$$\dot{m}_{lc} = \frac{2\pi\rho_l g (\rho_l - \rho_v) \delta_{L_c}^3}{\mu_l} \left[\frac{r_i}{3} - \frac{5\delta_{L_c}}{24} \right]. \quad (3)$$

It is important to note that the properties of the liquid are evaluated at the average temperature between the wall and the vapor.

3.2. Adiabatic section

The equations derived from the Nusselt analysis are not applied in the adiabatic section, because there is no radial heat transfer in this region. The axial heat conduction is relatively small due the small thickness and the low thermal conductivity of the material of the wall. Then, the thickness of the liquid film is considered constant and invariable in this region.

3.3. Evaporator

In the evaporator section, the vapor temperature is considered smaller than the wall temperature. The film thickness in the evaporator ($\delta_{La+Lc+\Delta x}$) and the film mean heat transfer coefficient (\bar{h}_{ef}) are calculated using the same Nusselt's model of condensation at a plain vertical surface and are given by the following equations, respectively:

$$\delta_{L_a+L_c+\Delta x} = \left[\delta_{L_a+L_c}^4 + \frac{4k_l \mu_l (T_{sat} - T_w)(x - L_a - L_c)}{g \rho_l (\rho_l - \rho_v) h_{lv}} \right]^{1/4}, \quad (4)$$

where $\delta_{L_a+L_c}$ is the film thickness at the end of the adiabatic section, and

$$\bar{h}_{ef} = \frac{g \rho_l (\rho_l - \rho_v) h_{lv}}{3\mu_l (T_v - T_w)(L_e - L_p)} \left[\left(C_1 (L_t - L_p) + \delta_{L_c+L_a}^4 - C_1 (L_c + L_a) \right)^{3/4} - \delta_{L_c+L_a}^3 \right], \quad (5)$$

where $C_1 = 4k_l \mu_l (T_{sat} - T_w) / g \rho_l (\rho_l - \rho_v) h_{lv}$.

In the region of the liquid pool, nucleate boiling is considered. Some correlations of the pool mean heat transfer coefficient have been obtained from the literature such as those of Shiraishi et. al (Shiraishi et. al apude Ong [7]) and Rohsenow (Rohsenow apude Noie [8]), given, respectively, by:

$$\bar{h}_{ep} = 0,32 \left[\frac{\rho_l^{0,65} k_l^{0,3} c_{pl}^{0,7} g^{0,2}}{\rho_v^{0,25} h_{lv}^{0,4} \mu_l^{0,1}} \right] \left(\frac{P_{sat}}{P_{atm}} \right)^{0,23} q_e^{0,4}, \quad (6)$$

and

$$\bar{h}_{ep} = \frac{q_e^{2/3}}{\frac{C_{sf} h_{iv}}{c_{pl}} \left\{ \frac{1}{h_{iv} \mu_l} \left(\frac{\sigma}{g[\rho_l - \rho_v]} \right)^{1/2} \right\}^{0.33} Pr} . \quad (7)$$

The C_{sf} is the Rohsenow constant obtained from the experimental data. Values for C_{sf} were suggested by Pioro [9] which can be applied for some specific combination between fluid and material of the wall.

The average heat transfer coefficient of evaporator is computed as a weighed mean of the heat transfer coefficients of film and pool, as show by the following equation:

$$\bar{h}_e = \frac{\bar{h}_{ep} L_p + \bar{h}_{ef} L_f}{L_e} . \quad (8)$$

3.4. Region of Vapor

This region encompasses the nucleus of evaporator, condenser and adiabatic section, where the vapor is found, which is assumed to be saturated and at the same temperature level along the pipe. Peterson [13] presents a model for the vapor pressure distribution inside the tube, which can be applied to the vapor region of thermosyphons, but in the present simplified case, no pressure or temperature distribution is considered. Vapor entrainment in any of the thermosyphon regions, due to liquid drag forces, is not considered, or, in other words, no shear stresses are modeled, in accordance with Nusselt's model. Therefore, all the vapor produced in the evaporator is considered condensed in the condenser.

3.5. Non-condensable gases region

The present model also considers the non-condensable gases which can be eventually found inside the thermosyphon. These gases are clustered in the upper part of the pipe during operation, decreasing the effective length of the thermosyphon. The heat transfer coefficient, in the presence of non-condensable gases, is significantly smaller when compared to the remaining region, where the condensation takes place. In this work, this region is considered adiabatic because the non-condensable gases avoid the heat transfer between the region they reside and the environment.

For modeling this region, the pressure, the mass and the temperature of these gases in the start up conditions are considered known. In steady state conditions, the final volume of the non condensable gases are obtained from the ideal gases law ($PV=nRT$), considering that the temperature of the gas is known as well as the pressure, which is considered the same as the vapor pressure in the upper part of the condenser region. The major problem is to determine the amount of non-condensing gases present inside the thermosyphon. As the tube is evacuated before the fluid is inserted in the cleaned tube, the non-condensable gases which eventually is found in this region, normally is formed by the chemical reaction between the fluid and the tube material. The volume of non-condensable gases formed by this way is hard to predict. Actually, this region is included in the present model to help in the adjustment of the theoretical model to experimental data that will be eventually available..

3.6. Distribution of temperature in the wall

The temperature distribution of the thermosyphon wall is determined through the method of Finite Volumes [10]. In this method, the wall is divided into several small volumes and a balance of energy, for steady state conditions, is performed in each volume, as illustrated in Fig. 3. The volume (Fig.3), with temperature " T_p ", is submitted to the following heat flux (q) through the areas in the boundaries: conduction for north (n) and south (s) sides and convection for east (e') and west (w') side. The outside and inside temperature of the volume are respectively T_o and T_i , where T_o is the environment temperature, considered uniform for each section, while T_i is assumed as the average between wall temperature and the vapor temperature, which, in turn, is considered constant

for each of the three regions. The following finite volume equation resulted from this balance, for each volume of length Δx , located at the x position (the axis origin, $x = 0$, is located in the top tube position):

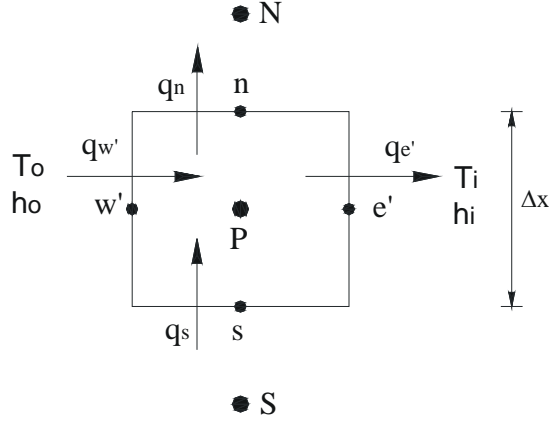


Figure 3 – Control Volume to the Balance Energy

$$A_p T_p = A_n T_N + A_s T_S + B, \quad (9)$$

where the coefficients are given by:

$$A_p = h_{w'} A_{w'} + A_s + A_n + h_e A_{e'}, \quad (10)$$

$$A_s = \frac{k_w A_{xs}}{\Delta x}, \quad (11)$$

$$A_n = \frac{kA_{xn}}{\Delta x}, \quad (12)$$

and

$$B = h_{w'} A_{w'} T_o + h_e A_{e'} T_i, \quad (13)$$

Equation 9 is applied to each thermosyphon wall control volume. All the equations together form a system of linear equations, which is solved by means of interactive methods. An initial temperature guess is applied to all the volumes and the temperature, for the $k+1$ iteration, is related to k iteration temperature by the following self adjustable equation, according to the Gauss-Seidel [10] method:

$$A_p T_p^{k+1} = A_s T_S^{k+1} + A_n T_N^k + B. \quad (14)$$

The heat transfer coefficient inside the tube depends of the thermosyphon region under consideration. For the condenser and the adiabatic section, the equations, as shown above, are used. For the evaporator, two sub regions are found: the pool and the falling liquid film. Therefore, Eq. 5, for the falling liquid sub region and Eq. 6 or 7 (the model uses the Eq. 7), for the pool sub-region are used, depending on whether the volume is in contact with the falling film or with the pool. The wall outside face receives uniform heat flux rate (Q_w), and Eq. 10 turns to be:

$$A_p = A_s + A_n + h_i A_e, \quad (15)$$

while B is given by:

$$B = Q_w' + h_i A_e T_i, \quad (16)$$

where Q_w' is the heat transfer rate.

3.7. Numerical solution

As already mentioned, the model is solved numerically by means of an iterative process, using FORTRAN. The input data for the model are: lengths of condenser (L_c), adiabatic section (L_a) and evaporator (L_e); mass of sodium (M_s), external heat transfer coefficient (h_{ext}), condenser external wall temperature (T_{ext}), tube inner diameter (D_i) and heat transfer rate (Q_e). The model determines the wall temperature distribution and the film thickness of the thermosyphon, for steady state conditions.

Figure 4 shows a schematic of the boundary conditions applied to the thermosyphon modeled in the present work. A known amount of heat, delivered to the evaporator section, leaves the device by convection in the condenser section. A small adiabatic section is considered. A non condensing gases region, located in the upper region of the condenser, is also considered,

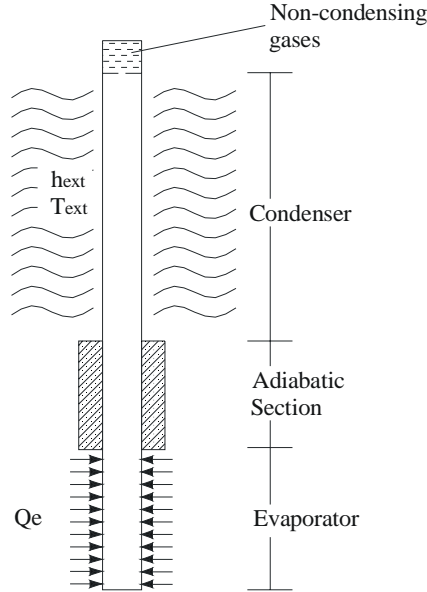


Figure 4 – Schematic of the boundary conditions applied to the thermosyphon modeled.

The control volume formulation of the heat transfer coefficients of the liquid film in the each control volume of condenser and evaporator walls were generated from the local coefficient of convection ($h_x = k/\delta$), which depends of the liquid film thickness [Eqs. 1 and 4]. Integrating the local heat transfer coefficient for each volume i of length Δx ($\Delta x = x(i) - x(i-1)$), results respectively, for the condenser and evaporator:

$$h_c(i) = \frac{4}{3} \frac{k_l}{C_1 \cdot \Delta x_c} \left((C_1 \cdot x(i))^{\frac{3}{4}} - (C_1 \cdot x(i-1))^{\frac{3}{4}} \right), \quad (17)$$

where: $C_1 = \frac{4 \cdot k_l \cdot \mu_l \cdot (T_v - T_w(i))}{g \cdot \rho_l \cdot (\rho_l - \rho_v) \cdot h'_{lvc}}$ and $h'_{lvc} = h_{lv} + 0,68 \cdot cp_l \cdot (T_v - T_w(i))$, and:

$$h_e(i) = \frac{4}{3} \frac{k_l}{C_2 \cdot \Delta x_e} \left(\frac{\left(C_2 \cdot x(i) + \delta_{L_a+L_c}^4 - C_2 \cdot (L_a + L_c) \right)^{\frac{3}{4}}}{-\left(C_2 \cdot x(i-1) + \left(C_2 \cdot x(i-1) + \delta_{L_a+L_c}^4 - C_2 \cdot (L_a + L_c) \right) \right)^{\frac{3}{4}}} \right), \quad (18)$$

where $C_2 = \frac{4 \cdot k_l \cdot \mu_l \cdot (T_v - T_w(i))}{g \cdot \rho_l \cdot (\rho_l - \rho_v) \cdot h'_{lve}}$ and $h'_{lve} = h_{lv} + 0,68 \cdot cp_l \cdot (T_w(i) - T_v)$.

The external heat transfer coefficient in the condenser ($h_{ext.c}$) is given by the correlation of Zhukauskas (apud [6]), valid for $0,7 < Pr < 500$ and $1 < Re_D < 10^6$, which are valid for the present case (Pr and Re values are around 0.73 and 3708.6):

$$h_{ext.c} = C_{Zhu} Re_D^m Pr^n \left(\frac{Pr}{Pr_w} \right)^{1/4} \quad (19)$$

where C_{Zhu} , m and n are constant. This correlation is valid for external cross flow of a fluid through tubes. In this case, air is considered as a cooling fluid. According to the literature [6], for $Pr > 10$, $n = 0.36$ and for $Pr \leq 10$, $n = 0.37$, while the values of C_{Zhu} and m are, 0.51 and 0.5, respectively, for the values of Reynolds of this model. The Reynolds number Re_D , based on the external tube diameter and the Prandtl number Pr are related to the external air flow, while Pr_w is the value of Pr calculated in the wall temperature.

A correlation for the heat transfer coefficient for liquid metal pools for high temperature thermosyphons could not be found in the literature, even though Carey [12] presents a liquid metal pool correlation for an open cylinder, which will be studied later as a possible correlation to be used. For the present work, the heat transfer coefficient for the pool is estimated by means of the correlation of Rohsenow for nucleate boiling, which is given by Eq. 7.

The whole tube was initially considered at uniform temperature, approximately in the design working temperature level, which basically depends of the amount of heat that the device is supposed to transfer. The initial guess reduces the computational time so that the convergence is obtained after a few seconds of computer processing time. The convergence is obtained comparing the heat input and output. When these values are unbalanced, the vapor temperature, which is considered uniform along the whole tube, is adjusted: decreased, if the heat output is larger than the heat input or increased if the heat output is lower than the heat input.

4. Results

The model was implemented to determine the temperature distribution and the overall thermal resistance of a mercury- stainless steel thermosyphon. The input data used in the simulation is presented in Table 2

Only the remaining gases after the tube evacuation were considered as the non-condensable gases. Considering a remaining pressure of $100 Pa$ and using the perfect gas model (as already observed) the tube length occupied by the non-condensable gases is around $5 \cdot 10^{-5} m$. This length is actually negligible, and, therefore, the effective length of the thermosyphon, determined as the total length of the tube less the length occupied by the non-condensable gases is 1 m.

The length of pool is 0.1382 m, which is calculated considering the total volume of mercury less the amount of the condensed fluid volume, that flows over the inside face of the walls..

Table 2. Input data for the numerical case study.

Inner diameter (D_i)	0.0239 m	Adiabatic section length (L_a)	0.06 m
Outer diameter (D_e)	0.0254 m	Outer temperature (condenser)	300 K
Heat transfer rate (Q_e)	580 W	Outside velocity of air (condenser)	2.3 m/s
Condenser length (L_c)	0.74 m	Mass of mercury	704.39 g
Evaporator length (L_e)	0.2 m		

Figure 5 shows the thickness profile of liquid film along the length of the tube. In this figure, it is possible to observe the increase of the film thickness along the tube length, from zero to a maximum thickness, at the interface between the condenser and the adiabatic sections. In the adiabatic region, where no heat transfer takes place, the film thickness does not increase. The thickness quickly decreases in the evaporator region, since the film is evaporated due to the heat externally applied. After the liquid film reaches the liquid pool, the film thickness is considered as of zero thickness. The film thickness profile is obtained using the wall temperature profile shown in Fig. 6. Actually, the temperature profile is almost uniform, with a difference of only approximately 0.17°C between the condenser and the liquid pool of the evaporator. In the adiabatic section, there is a linear variation of this temperature, as only conduction heat transfer takes place in this region. The small temperature decrease observed in the condenser region can be explained by the fact that the model considers that the vapor is at a uniform temperature, represented by the horizontal line in Fig. 6, which is not an exact hypothesis, as already observed in this work. The Nusselt model for condensation and evaporation over vertical surfaces shows that the convection heat transfer coefficient is dependent on the film thickness, and its variation with the tube length is shown in the plot presented in Fig. 7. As the material of the tube, stainless steel, has a low thermal conductivity and as the heat transfer coefficient between the vapor and the film thickness is very high, the temperature of the tube wall decreases from the rear end to the adiabatic region. As already mentioned, the temperature of the vapor is adjusted in each numerical model run..

The very small difference, between the vapor and the wall temperatures, leads to increase of the value of the coefficient of heat transfer, as one can observe in Eqs. 2 and 5. Despite of the fact that the coefficient of heat transfer increases with the decreasing film thickness, the temperature of the wall in the evaporator section, which is not in contact with the pool, presents the same trend of the condenser because in this case, heat is being added to the wall, while, in the condenser case it is being removed. But the temperature variation within each section is so small that it can be considered uniform for practical purposes. Other cases, considering a thicker wall with a high conductance material (copper) were simulated and the decrease in the evaporator wall temperature was not observed, while in the condenser the temperature still decreases very little. Some experimental results for liquid metal heat pipes, such as the work of Yamamoto et al[5] shows that these effects were not expected in actual data which means that the model should be revised and experimental data should be obtained for thermosyphons and compared with the proposed model.

It is also observed in Fig. 6, that the temperature of the wall region in contact with the liquid pool is larger than that for the region in contact with the liquid film. This difference of temperature between liquid film and pool is justified by the heat transfer coefficient. The heat transfer coefficient of the liquid film is of the order of $3.64 \times 10^5 \text{ W/m}^2\text{K}$, larger than that for the pool (given by Rohsenow correlation), of $2.27 \times 10^5 \text{ W/m}^2\text{K}$. It is important to remember that no pool liquid model correlations are available in the literature for thermosyphons and that a correlation obtained for other liquids were applied in this paper. The linear profile observed in the adiabatic region is due to the hypothesis that no heat is exchanged with the environment.

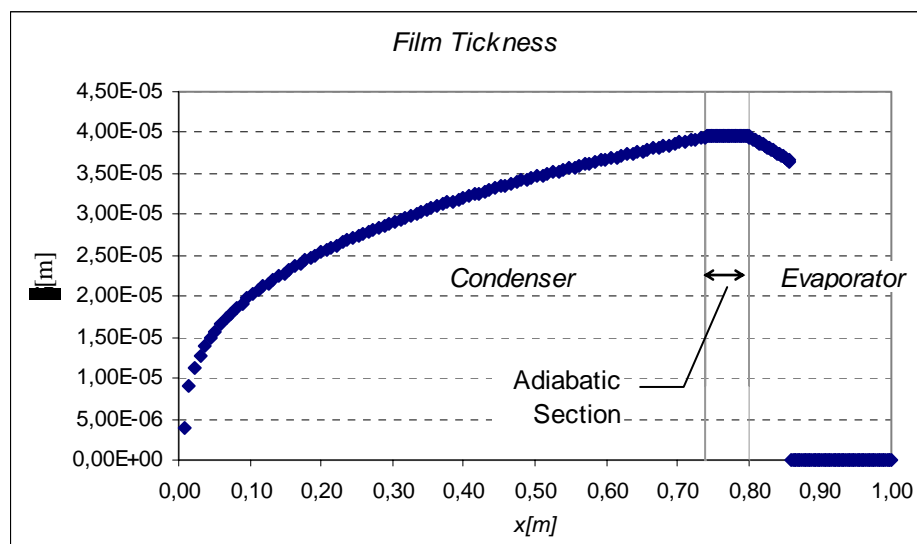


Figure 5 – Film thickness of thermosyphon along the thermosyphon length.

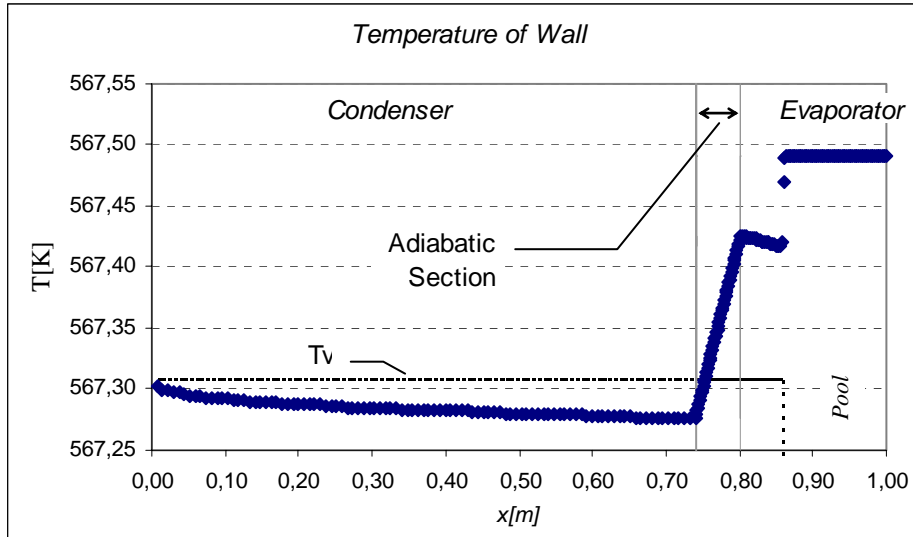


Figure 6 – Wall temperature of thermosyphon.

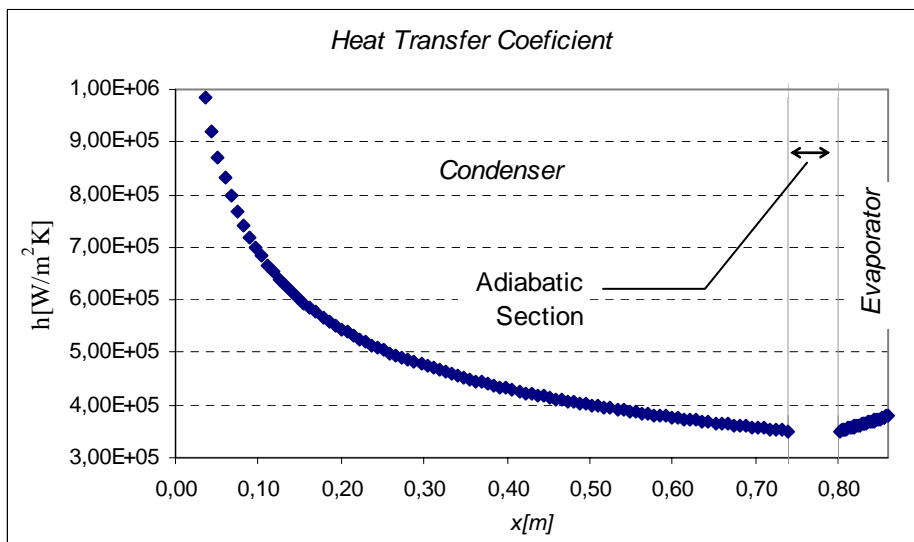


Figure 7. Liquid film heat transfer coefficient as a function of the tube length.

Figure 8 shows the overall thermal resistance of the thermosyphon tested as a function of the heat power to be transported. The increase in the heat power decreases the overall thermal resistance. Actually, the variation of the overall resistance is small, and can be considered constant for most of the practical applications.

Figure 9 shows the power input heat transfer as a function of the thermosyphon temperature level, defined as the mean temperature of the adiabatic section. In this figure, it can be observed that the higher the power to be transferred, the higher is the temperature level of the device.

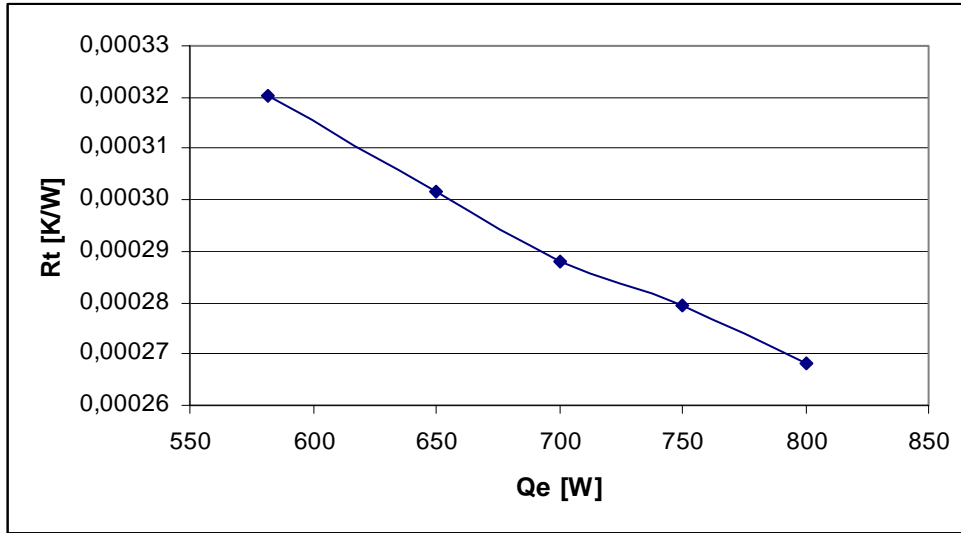


Figure 8 – Thermal resistance versus Heat transfer rate.

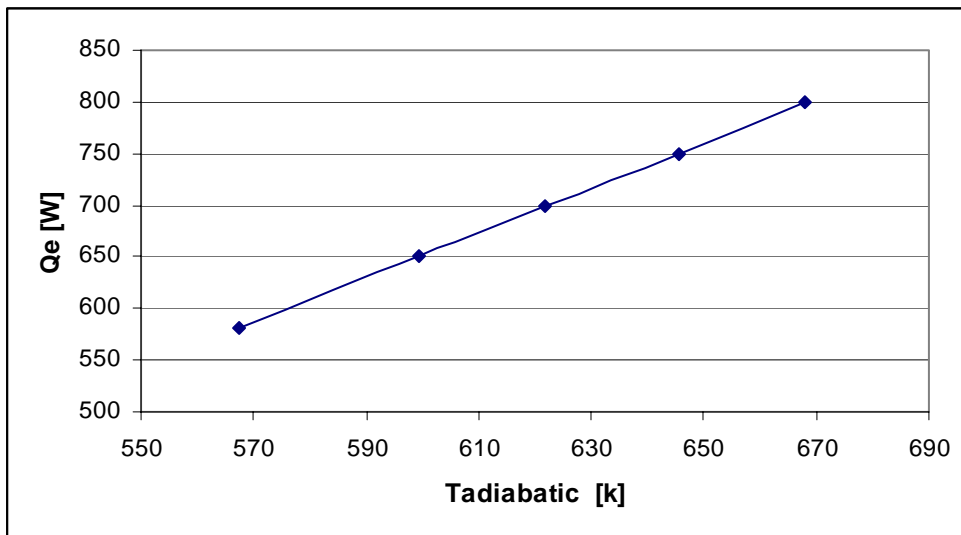


Figure 9 – Heat transfer rate versus temperature of adiabatic section.

5. Conclusion

This paper shows a steady state model, developed for a high temperature thermosyphon, where the working fluid is liquid metal. The thermosyphon is divided into seven main regions, each one modeled separately. The wall is divided into several control volumes. A heat balance is performed for each volume, so that the variation of the coefficient of heat transfer, both for the evaporator and for the condenser is taken into account. The vapor temperature, which is considered uniform along the tube, is updated in each iterative run step, until convergence. Nusselt condensation and evaporation models for vertical walls were applied. The resulting coefficients of heat transfer show very high values due to two main reasons: the high thermal conductivity properties of the working fluid and the very small differences between the vapor and the wall temperatures. Results in the literature for heat

pipes shows that these values are probably over dimensioned. Therefore, one can conclude that the model still needs adjustments, such as:

- Introduction of a shear stress coefficient in the convection heat transfer Nusselt model (see Faghri [1],
- Introduction of a vapor model, where the pressure and the temperature level of the vapor changes according to the region of the thermosyphon,
- Adaptation and introduction of a liquid metal pool model based on literature models such as the one presented by Carey [12], for liquid metal pools in open cylinders.

After the model is concluded, experimental results, to be obtained in the Heat Pipe Laboratory (LABTUCAL) will be compared with the model and, according to the comparison, new correlations for the convection heat transfer coefficient in the condenser and evaporator, as well as in the liquid metal pool, could be proposed. The model will also receive adjustments at this time. The experimental set up is under tests, but no results are available in the moment.

The present model is an important tool to be used in the design of high temperature thermosyphons, for several applications such as in heat exchangers for petroleum industry.

6. Acknowledgments

This work, develop in the Heat Pipe Laboratory (LABTUCAL) is funded by the National Council for Scientific and Technological Development (CNPq) and by the Foundation of Support to the Scientific and Technological Research of Santa Catarina State (FAPESC). We gratefully acknowledge the support of the Department of Mechanical Engineering (EMC) of Federal University of Santa Catarina (UFSC).

References

- [1] Faghri, A., "Heat Pipe Science and Technology", Taylor and Francis, Washington, 1995.
- [2] Dunn, P. D., and Reay, D. A., "Heat Pipes", 3rd ed., Pergamon Press, Oxford, 1982.
- [3] Storey, J. Kirk, "Modeling the Transient Response of a Thermosyphon", Ph. D. Thesis, Department of Mechanical Engineering, Brigham Young University, December, 2003.
- [4] Reed, J. G. and Tien, C. L., "Modeling of the Two-Phase Closed Thermosyphon", Transactions of the ASME, vol. 109, August, 1987.
- [5] Yamamoto, T.; Nagata, K.; Katsuta, M. and Ikeda, Y., "Experimental Study of Mercury Heat Pipe", Experimental Thermal and Fluid Science, vol. 9, pp. 39-46, 1994.
- [6] Incropera, Frank. P. and Witt, David P., "Fundamentos de Transferência de Calor e de Massa", 5^o ed., ed. LTC , Rio de Janeiro, RJ, 2002.
- [7] Ong, K. S., "A Simple Theoretical Model of a Thermosyphon", The 7th International Heat Pipe Symposium, October 12-16, Jeju, Korea, 2003.
- [8] Noie, S. H.; Kalaei, M. H. and Khoshnoodi, M., "Experimental Investigation of a Two Phase Closed Thermosyphon", The 7th International Heat Pipe Symposium, October 12-16, Jeju, Korea, 2003.
- [9] Pioro, I. L., "Experimental evaluation of Constants for the Rohsenow Pool Boiling Correlation", International Journal of Heta Transfer and Mass, vol. 42, pp. 2003-2013, 1999.
- [10] Maliska, Clovis R., "*Transferência de Calor e Mecânica dos Fluidos Computacional*", Livros Técnicos e Científicos Editora, 1995.
- [11] Renken, W. A. and Lundberg, L. B., "High Temperature Heat Pipes for Terrestrial Applications", 3rd International Heat Pipe Conference, California, May 22-24, 1978.
- [12] Carey, V. P., "Liquid-vapor phase-change phenomena: an introduction to the thermophysics of vaporization and condensation processes in heat transfer equipment", Taylor and Francis, Bristol, 1992.
- [13] Peterson, G. P., "An Introduction to Heat Pipe: Modeling, Testing and Applications", John Wiley&Sons. Inc., New York, 1994.